International Journal of Coal Science & Technology (2024) 11:15
https://doi.org/10.1007/s40789-024-00663-3

RESEARCH

Comprehensive kinetic study on ammonia/ethylene counter-flow diffusion flames: influences of diluents

Zhimei Shu[1,2] · Tingting Xu[1,2] · Jiayi Xiao[1,2] · Qige Deng[1,2] · Xuan Zhao[1,2] · Tianjiao Li[1,2] · Yaoyao Ying[1,2] · Dong Liu[1,2]

Received: 7 December 2022 / Revised: 13 July 2023 / Accepted: 22 January 2024

Abstract
This study aimed to investigate the effects of ammonia addition on ethylene counter-flow diffusion flames with different diluents on the fuel or oxidizer side, using kinetic analyses. A special emphasis was put on assessing the coupled chemical effects of NH_3 and CO_2 on C_2H_4 combustion chemistry. The chemical effects could be evaluated by comparing fictitious inert NH_3 or CO_2 with normal active NH_3 or CO_2. The results revealed that the addition of NH_3 decreased the mole fractions and production rates of key soot precursors, such as acetylene, propynyl, and benzene. When CO_2 was used as the dilution gas, the coupled chemical effects of NH_3 and CO_2 were affected by the chemical effects of CO_2 to varying degrees. With the oxidizer-side CO_2 addition, the coupled chemical effects of NH_3 and CO_2 reduced the mole fractions of H, O, OH radicals, acetylene, propynyl, and benzene, while the effects differed from the fuel-side CO_2 addition. The coupled chemical effects of NH_3 and CO_2 also promoted the formation of aldehyde contaminants, such as acetaldehyde, to some extent, particularly with CO_2 addition on the oxidizer side.

Keywords Ammonia addition · Diluents · Coupled chemical effects · Kinetic analysis

1 Introduction

The goal of reducing carbon emissions had been pursued by various countries in recent years. However, the energy structure was still dominated by fossil fuels, whose incomplete combustion could inevitably generate the production of pollutants such as NO_x, carbon oxides, and harmful soot particles. The soot could reduce the efficiency of combustion, damage the environment, and endanger human health (Wang 2011; Dong et al. 2023). Therefore, it was important to explore technologies that could reduce dependence on fossil fuel sources, such as renewable energy sources and carbon-free fuel combustion.

Ammonia (NH_3) could be a viable clean fuel, with a 2018 report in the journal of Science lauding it as "liquid sunlight" that would provide a renewable, carbon-free energy source (Service 2018). NH_3 also had potential benefits and technical advantages as a sustainable fuel for power generation on vehicles. In particular, NH_3 was more effective than other fuels, had a longer driving range, and was more compact and cost-effective (Zamfirescu and Dincer 2009). Additionally, the octane rate of NH_3 was high, reaching about 110–130 (Sonker et al. 2022). The applications of NH_3 as fuel in gas turbines, pulverized coal co-combustion and industrial furnaces have been very successful in recent years (Kobayashi et al. 2019).

Given ammonia flame instability and low combustion intensity (Lhuillier et al. 2020; Zhou et al. 2021), researchers have been motivated to study its mixing with hydrocarbon fuels such as methane and ethylene (Chen and Liu 2023). Firstly, the combustion of the methane mixing ammonia (Grcar et al. 2004; Shu et al. 2021; Li et al. 2021) has been explored. It revealed that as the proportion of mixed NH_3 increased in the CH_4/NH_3 turbulent premixed flame, the maximum flame surface density decreased, leading to

✉ Tingting Xu
tingtingxu1225@126.com

✉ Dong Liu
dongliu@njust.edu.cn

1 MIIT Key Laboratory of Thermal Control of Electronic Equipment, School of Energy and Power Engineering, Nanjing University of Science and Technology, Nanjing 210094, China

2 Advanced Combustion Laboratory, School of Energy and Power Engineering, Nanjing University of Science and Technology, Nanjing 210094, China

Published online: 15 March 2024

a decrease in the ratio of the turbulent combustion velocity of NH_3 to the unstretched laminar combustion velocity (Ichikawa et al. 2019). The primary way in which ammonia affected the velocity of the CH_4/NH_3 flame was by altering the concentration of H and OH radicals. The sensitivity of flame to stretch increased with equivalence ratio and NH_3 concentration (Okafor et al. 2018). Secondly, ethylene (C_2H_4), as the simplest alkene, has been established its detailed combustion reaction mechanism. For microgravity ethylene diffusion flames, researchers (Lecoustre et al. 2012) have evaluated experimentally and numerically that soot formation occurred in regions where the C/O atom ratio and temperature exceeded critical values of 0.53 and 1305 K, respectively. Moreover, the local C/O atomic ratio associated with soot incipience was lower in terrestrial gravity, falling within the range of 0.32 to 0.44 (Frolov et al. 2023). The carbon atom number and C/H ratio of the final soot particles in ethylene combustion were approximately twice that of methane combustion (Wang et al. 2021). Therefore, the soot production in ethylene turbulent flames after nitrogen was replaced by hydrogen or ammonia was studied (Boyette et al. 2021). It was found that hydrogen substitution increased soot production, while ammonia addition inhibited soot formation. Additionally, the replacement of some Ar by NH_3 in ethylene premixed flame was responsible for the decrease of the maximum mole fractions of C_4H_2 and C5 to C10 species (Renard et al. 2009). In the C_2H_4 diffusion flame, it was revealed that NH_3 delayed and suppressed the formation of polycyclic aromatic hydrocarbons (PAHs), and NH_3 had a greater reduction influence than Ar (Ren et al. 2022). By some kinetic studies, some researchers also found that doping ammonia decreased soot particle size, the volume fraction of soot particles and the mole fractions of soot precursors both in laminar premixed (Shao et al. 2022) and diffusion (Liu et al. 2021; Zhang et al. 2023) ammonia/ethylene flames. Then through the kinetic analyses of the mole fractions of typical soot precursors (Deng et al. 2022), it was found that NH_3 addition inhibited the production of important precursor polycyclic aromatic hydrocarbons, which was mainly due to the chemical effects of NH_3 in C_2H_4/NH_3 diffusion flame. Furthermore, the soot from ethylene/ammonia laminar flames was experimentally and numerically studied, and found that the reduction of soot formation was mainly due to the chemical effects of NH_3 (Bennett et al. 2020). However, it was not completely separate the chemical effect of NH_3 from its thermal and dilution effects (Liu et al. 2015a). It could be concluded that mixing ammonia with traditional hydrocarbon fuels improved the combustion properties of ammonia and inhibit the formation of soot precursors. However, it was not clear what factors will affect the chemical effects of NH_3 on C_2H_4 combustion chemistry, such as different diluents.

It had been found that different diluent gas could affect the reaction kinetics and change the thermophysical properties of the mixture such as specific heats, diffusion coefficients, etc. to change the combustion temperature or reduce the generation of pollutants (Vancoillie et al. 2013; Chen et al. 2022). Researchers (Yelverton and Roberts 2008) have measured the soot surface temperature in pure and diluted ethylene co-flow diffusion flames, using helium (He), argon (Ar), nitrogen (N_2), or carbon dioxide (CO_2) individually. It revealed that the addition of a diluent cooled the soot surface. The He-diluted flames were the warmest and the CO_2-diluted flames were the coolest. In addition, the sensitivity of the DME flame velocity to the H-atom production and consumption reactions also decreased with the dilution of CO_2. In the lean DME flame, both the inert third-body effect and the kinetic effect of CO_2 reduced the H-atom production. For the rich DME flame, the inert third-body effect increased the formation of H-atom by inhibiting the kinetic effect of CO_2 (Liu et al. 2013). Focusing on the soot formation in CO_2-diluted environments, researchers performed experiments on ethylene fuel pyrolysis with varying levels of CO_2 dilution and found that 25% CO_2 tended to increase soot production while a higher level of CO_2 reduced soot formation (Abián et al. 2012). In laminar co-flow C_2H_4/air diffusion flames, it concluded that the concentrations of the critical soot formation species, including H, C_2H_2, benzene, and pyrene were lowered in the CO_2-diluted flames due to the additional chemical effects of CO_2. CO_2 remained more effective than N_2 as a diluent to suppress soot formation at elevated pressures (Liu et al. 2015). The chemical effects of adding CO_2 to the fuel side or oxidant side were simulated in countercurrent ethylene/air diffusion flame, and it concluded that CO_2 could suppress soot formation by lowering both temperature and acetylene concentration and enhancing the concentration of OH radical (Liu et al. 2001).

It may be concluded that the combustion atmosphere had very significant influences on the combustion process. However, most of the available studies have focused on the effects of diluents on the combustion of hydrocarbon fuels. The studies of the effects of diluents on ethylene/ammonia counter-flow diffusion flames were limited. Therefore, the aim of this paper was to investigate the combustion chemistry of C_2H_4/NH_3 with various diluents via chemical kinetics analyses. The chemical effects of NH_3 addition on the flame temperature, typical radical species, and important intermediate species were analyzed, with particular attention to the coupled chemical effects of NH_3 and CO_2 on the combustion process. The present study had the potential to give a better understanding of the fundamental ammonia combustion with different diluents, and to provide a reference for the detailed alteration of soot precursors and the control of other pollutant emissions.

2 Kinetic modeling and analysis method

The counter-flow diffusion flame simulations were performed using the CHEMKIN/OPPDIF module. The detailed chemical mechanism employed here was KM2-G, which involved 202 species and 1351 reactions (Wang et al. 2013). The KM2-G mechanism coupled a comprehensive model for nitrogen chemistry with the KM2 hydrocarbon-PAH mechanism (Zhou et al. 2022). The nitrogen chemistry included the oxidation of NH_3 and the formation of nitric oxide species, which have been well validated against experimental data (Glarborg et al. 2018). The KM2 mechanism was also shown to perform excellently in terms of the prediction of the first aromatic ring as well as soot formation (Wang et al. 2020).

The separation distance between the two nozzles of the counter-flow diffusion flame burner was 8 mm. With the pressure condition of 1 atm, the inlet velocities of the fuel and oxidizer were set at 25 cm/s, and the initial temperature was 300 K. Considering that N_2 was unstable at high temperatures, and could produce thermal NO_x that affected the combustion chemistry of NH_3. Therefore, as the basic working condition, the fuel side consisted of 80% C_2H_4 + 20% Ar, and the oxidizer side was 21% O_2 + 79% Ar. Then He and CO_2 replaced the diluent gas Ar on the fuel side or the oxidizer side. Additionally, the coupled chemical effects of NH_3 and CO_2 were further analyzed by introducing the fictitious inert CO_2 and NH_3. The specific working conditions were shown in Tables 1 and 2. In Table 1, F1–F5 represented the conditions of the C_2H_4/NH_3 flames with Ar dilution and different NH_3 additions. F6–F10 and F11–F15 illustrated the conditions of the C_2H_4/NH_3 flames with He dilution on the fuel side and oxidizer side, respectively, and different NH_3 additions. In Table 2, F1–F9 outlined the conditions of the C_2H_4/NH_3 flames with CO_2 dilution on the fuel side and various NH_3 additions, F10–F18 delineated the conditions of the C_2H_4/NH_3 flames with CO_2 dilution on the oxidizer side and various NH_3 additions.

As the effects of additives on fuel combustion were divided into three types: (1) dilution effects resulting from the decrease of reactive species mole fractions and collision frequencies, (2) thermal effects as a result of flame temperature variation, and (3) chemical effects caused by the participation of additives in chemical reactions (Du et al. 1990).

These three effects were highly coupled which made it quite difficult to discuss them separately. Therefore, the fictitious species method, which was firstly proposed by Liu et al. (2001) and had been employed by many researchers to analyze the specific effects of additives in different flames (as shown in Table 3), could isolate the chemical effects of additives from the dilution and thermal effects. In the study, in order to identify the coupled chemical effects of NH_3 and CO_2, normal active CO_2 (denoted as CO_2) and fictitious inert CO_2 (denoted as FCO_2) were also introduced for comparisons (Liu et al. 2003, 2015; Gu et al. 2016; Naseri et al. 2017). Similarly, the normal active NH_3 was denoted as NH_3, and the fictitious inert NH_3 was denoted as FNH_3. Although the fictitious species could not be directly added to real flames, in the numerical strategy, FCO_2 and CO_2 had the same thermodynamic parameters, transport parameters, and third-body collision efficiency, and the only difference was that FCO_2 did not participate in any relevant chemical

Table 1 Detailed flame conditions with Ar and He dilution (Unit for reactants is mole fractions)

No.	Fuel side					Oxidizer side		
	C_2H_4	Ar	He	NH_3	FNH_3	O_2	Ar	He
F1	0.8	0.2				0.21	0.79	
F2	0.6	0.2		0.2		0.21	0.79	
F3	0.6	0.2			0.2	0.21	0.79	
F4	0.4	0.2		0.4		0.21	0.79	
F5	0.4	0.2			0.4	0.21	0.79	
F6	0.8		0.2			0.21	0.79	
F7	0.6		0.2	0.2		0.21	0.79	
F8	0.6		0.2		0.2	0.21	0.79	
F9	0.4		0.2	0.4		0.21	0.79	
F10	0.4		0.2		0.4	0.21	0.79	
F11	0.8	0.2				0.21		0.79
F12	0.6	0.2		0.2		0.21		0.79
F13	0.6	0.2			0.2	0.21		0.79
F14	0.4	0.2		0.4		0.21		0.79
F15	0.4	0.2			0.4	0.21		0.79

Table 2 Detailed flame conditions with CO_2 dilution (Unit for reactants is mole fractions)

No.	Fuel side							Oxidizer side		
	C_2H_4	Ar	CO_2	FCO_2	NH_3	FNH_3	(Oxidizer side) O_2	Ar	CO_2	FCO_2
F1	0.8		0.2				0.21	0.79		
F2	0.6		0.2		0.2		0.21	0.79		
F3	0.6		0.2			0.2	0.21	0.79		
F4	0.6			0.2	0.2		0.21	0.79		
F5	0.6			0.2		0.2	0.21	0.79		
F6	0.4		0.2		0.4		0.21	0.79		
F7	0.4		0.2			0.4	0.21	0.79		
F8	0.4			0.2	0.4		0.21	0.79		
F9	0.4			0.2		0.4	0.21	0.79		
F10	0.8	0.2					0.21		0.79	
F11	0.6	0.2			0.2		0.21		0.79	
F12	0.6	0.2				0.2	0.21		0.79	
F13	0.6	0.2			0.2		0.21			0.79
F14	0.6	0.2				0.2	0.21			0.79
F15	0.4	0.2			0.4		0.21		0.79	
F16	0.4	0.2				0.4	0.21		0.79	
F17	0.4	0.2			0.4		0.21			0.79
F18	0.4	0.2				0.4	0.21			0.79

reactions. In this way, the dilution and thermal effects, which were similar and commonly both be classified as pure physical effects, were consistent. While the chemical effects of CO_2, which not only affected the main combustion products (CO, H_2) but also could play an important role in soot evolution, could be isolated (Zhao and Liu 2022). It could be considered that the variation of the flame temperatures and species concentration between the FCO_2 and the CO_2 flames was purely caused by the chemical effects. The similar method was also used for NH_3. The differences between the results from NH_3 and FNH_3 additions were attributed to the NH_3 chemical effects, and the coupled chemical effects of NH_3 and CO_2 could be suggested from the differences between the CO_2/NH_3 and FCO_2/FNH_3 flames (Liu 2014; Li et al. 2015; Ying and Liu 2015; Liu 2015a; Luo and Liu 2017; Pan and Liu 2017; Deng et al. 2022; Zhao and Liu 2022).

3 Results and discussion

3.1 With Ar or He dilution

The effects of NH_3 addition on the flame temperature, major species, free radicals and important intermediate species with Ar or He dilution were investigated, with emphasis on distinguishing the detailed effects of dilution, thermal and chemical effects of NH_3.

3.1.1 Flame temperature profiles

The effects of NH_3 with Ar or He dilution on the flame temperatures were shown in Fig. 1. The dilution and thermal effects of NH_3 resulted in temperature differences between 0% NH_3 and 20% FNH_3 additions, and the differences between 20% NH_3 and 20% FNH_3 additions were due to the chemical effects of NH_3. The combined influences of dilution, thermal, and chemical effects led to the differences between 0% NH_3 and 20% NH_3 additions. For clarity of exposition, the specific effects were marked in Fig. 1.

In Fig. 1, the chemical effects of NH_3 increased the flame temperature, whereas the dilution and thermal effects of NH_3 caused the temperature to decrease. Consequently, the flame temperature was reduced due to the dilution and thermal effects of NH_3, which had a more pronounced influence on the flame temperature than the chemical effects. The data in Fig. 1c showed that when He replaced Ar on the oxidizer side, the peak flame temperature was slightly lower, which may be due to the higher thermal diffusivity of He (Yelverton and Roberts 2008).

Table 3 Summary of the studies using fictitious species to isolate the chemical effects

Reference	Fuel and burner types	Additives	Results
Liu et al. (2001)	Ethylene counter-flow diffusion flames	FCO_2	The chemical effects of CO_2 addition reduced concentration of acetylene and flame temperature and conversion of carbon dioxide by hydrogen atom to hydroxyl
Park et al. (2003)	H_2-O_2 counter-flow diffusion flames	$X(CO_2)$	Chemical effects due to thermal dissociation of added CO_2 caused the reduction flame temperature in addition to some thermal effects
Guo and Smallwood (2008)	Ethylene co-flow diffusion flames	XCO_2	The chemical effect of CO_2 addition was primarily caused by the reduced concentration of radical H, which suppressed the soot inception and surface growth rate
Liu (2014)	Premixed laminar low-pressure dimethyl ether flames	F-H_2/F-O_2	The chemical effects of H_2 addition caused the DME profile to move toward the upstream side and could suppress the production of acetylene and ethylene
Ying and Liu (2015)	Laminar premixed stoichiometric methane-air flames	F-H_2/F-O_2	Chemical effects of H_2 additive suppressed the formation of acetylene and ketene, and facilitated the productions of formaldehyde and acetaldehyde
Liu (2015b)	Premixed ethylene/ethanol flames	F-Ethanol	The ethanol chemical effects promoted formations of hazardous pollutants formaldehyde and acetaldehyde, and especially were responsible for the significant increase of acetaldehyde
Gu et al. (2016)	Axisymmetric laminar co-flow ethylene/air diffusion flames	FH_2/FCO_2	The chemical interactions between hydrogen and carbon dioxide on soot formation were weak
Naseri et al. (2017)	Premixed laminar ethylene/oxygen/argon burner stabilized stagnation flames	FCO_2	The addition of CO_2 reduced the concentrations of H, C_2H_2, C_6H_6, and large PAHs which all suppressed the soot formation process through a chemical effect
Pan and Liu (2017)	Laminar lean premixed dimethyl ether flames	FH_2/FCO_2	The coupled effects of H_2/CO_2 additions on major species, intermediate stable species and radicals were discussed and analyzed in detail
Mahmoud et al. (2019)	Ethylene counter-flow diffusion flames	FCO_2/FH_2O	The detailed chemical roles of CO_2 and H_2O at different stages of soot formation were numerically investigated
Deng et al. (2022)	Ethylene counter-flow diffusion flames	FNH_3	The flame temperature and the mole fraction profiles affected by the chemical effects of NH_3 addition for major species, free radicals, intermediate species, aromatics, and soot were analyzed

3.1.2 Major species and radicals

The mole fraction profiles of the fuel C_2H_4 with different NH_3 additions were shown in Fig. 2. The differences between the NH_3 addition and FNH_3 addition revealed that the chemical effects of NH_3 could slightly accelerate fuel consumption. In Fig. 2c, as He replaced Ar on the oxidizer side (F11–F15 conditions in Table 1), the profiles shifted toward the oxidizer side. To analyze the detailed consumption of C_2H_4, the C_2H_4 rates of production were performed in Fig. 3, it could be found that when the diluent was Ar (F1–F5 conditions in Table 1), C_2H_4 was mainly consumed by radicals, including $C_2H_4+H=C_2H_3+H_2$ and $C_2H_4+OH=C_2H_3+H_2O$ reactions. The rates of these reactions responsible for the depletion of C_2H_4 decreased with the addition of NH_3, which dominated the chemical effects. Therefore, it was necessary to analyze the mole fractions of these typical radicals, including H, O, and OH radicals.

Figure 4 gave the mole fractions of the H radical with different NH_3 additions. When the dilution gas was Ar (F1–F5 conditions in Table 1) or He (F6–F15 conditions in Table 1), the mole fractions of H radical decreased with increasing concentrations of NH_3 additive, and with 20% NH_3 addition, the chemical effects of NH_3 further reduced H concentration. While the blending ratio was 40%, the chemical effects of NH_3 increased the mole fraction of H radical when the dilution gas was only Ar (as shown in Fig. 4a). The results were consistent with Deng et al. (2022) and Zhang et al. (2023).

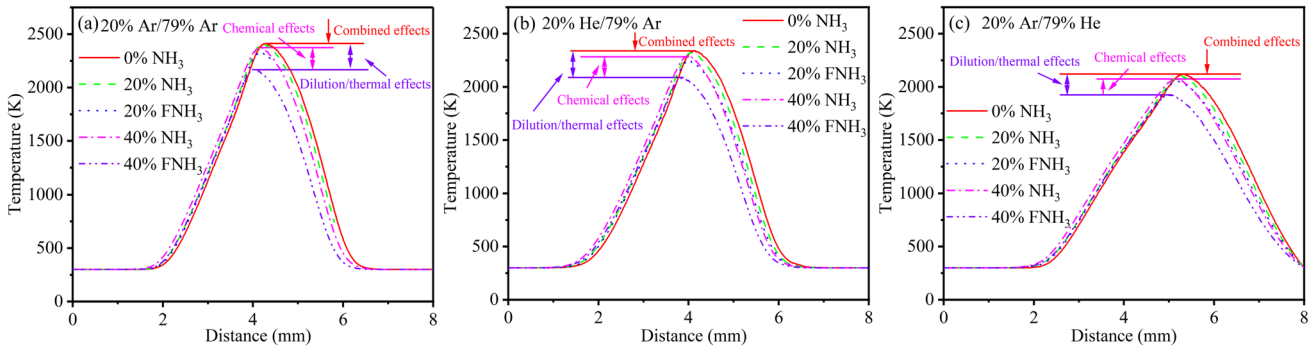

Fig. 1 Flame temperature with Ar or He dilution and different NH_3 additions. *Notes*: The 20% Ar/79% Ar represented the dilution gas was Ar both on the fuel side and the oxidizer side (F1-F5 conditions in Table 1). The 20% He/79% Ar and the 20% Ar/79% He represented dilution gas He replaced Ar on the fuel side (F6-F10 conditions in Table 1) and the oxidizer side (F11-F15 conditions in Table 1). The annotations for Figs. 2, 3, 4, 5, 6, 7, 8 and 9 have the same meanings, which will not be noted again in the following

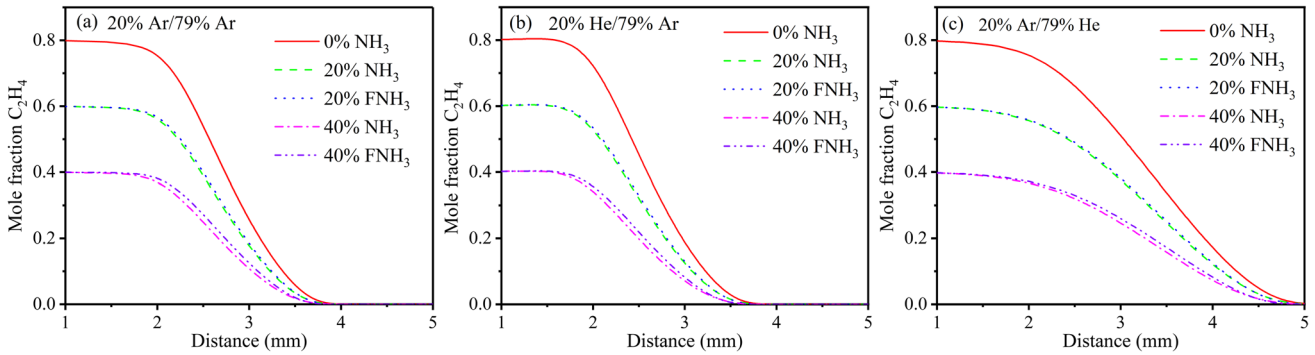

Fig. 2 Mole fraction profiles of C_2H_4 with Ar or He dilution and different NH_3 additions

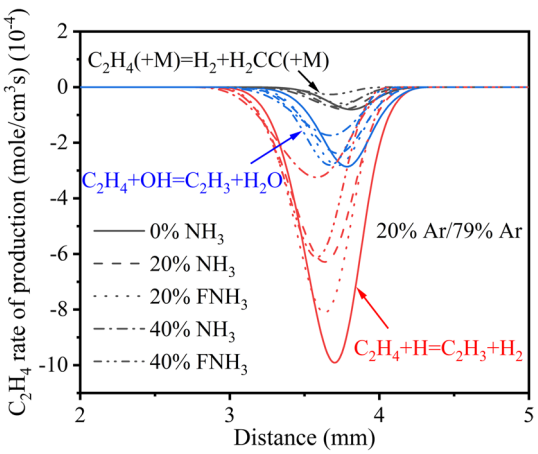

Fig. 3 Rate of production of C_2H_4 with different NH_3 additions

Oxidation of PAH and soot particles may occur subsequent to formation in diffusion flames and the main oxidation reactants were OH, O, and O_2 (Richter and Howard 2000). Therefore, it was necessary to analyze the mole fraction profiles of the O radical, which were shown in Fig. 5. Comparing the O radical mole fractions with NH_3 and FNH_3 additions, it illustrated that the chemical effects of NH_3 could inhibit the formation of O radical regardless of the different dilution gas.

Furthermore, hydroxyl OH played a dominant role in the soot generation area of counter-flow diffusion flame, due to the relatively low concentration of O_2. The OH radical was mainly oxidized by reacting with the active sites on the surface of soot, which could inhibit the further generation of soot (Frenklach et al. 2018). The mole fraction profiles were performed in Fig. 6. The addition of NH_3 also suppressed the formation of OH radical, but different from the effects on O, H radicals, it was primarily because of the dilution and thermal effects of NH_3, which were more pronounced than its chemical effects. Notably, the mole distributions of OH radical with NH_3 addition were higher than those with FNH_3 addition, indicating that the chemical effect of NH_3 promoted the formation of OH radical indeed.

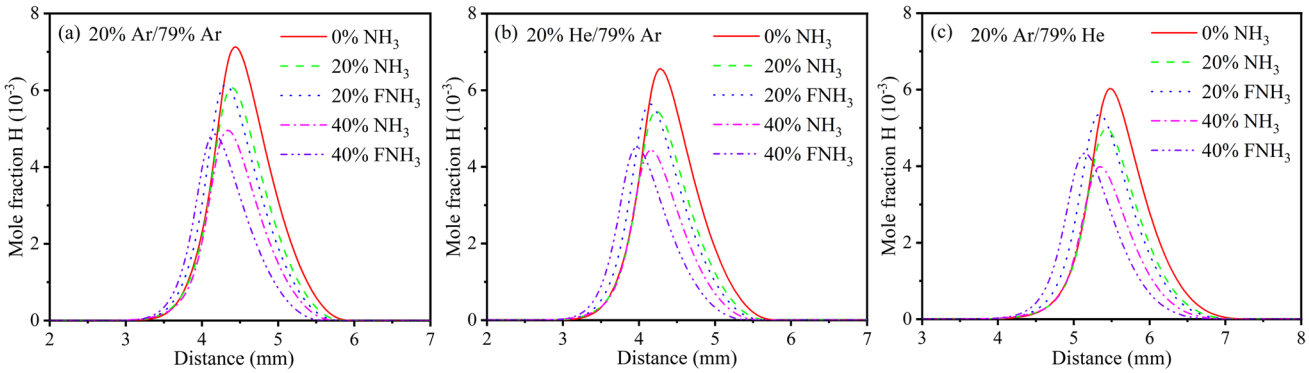

Fig. 4 Mole fraction profiles of H with Ar or He dilution and different NH_3 additions

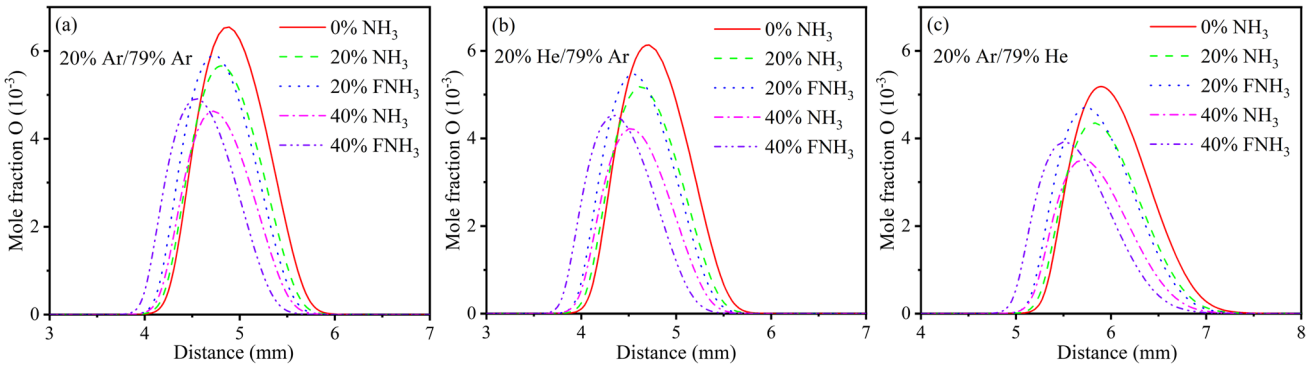

Fig. 5 Mole fraction profiles of O with Ar or He dilution and different NH_3 additions

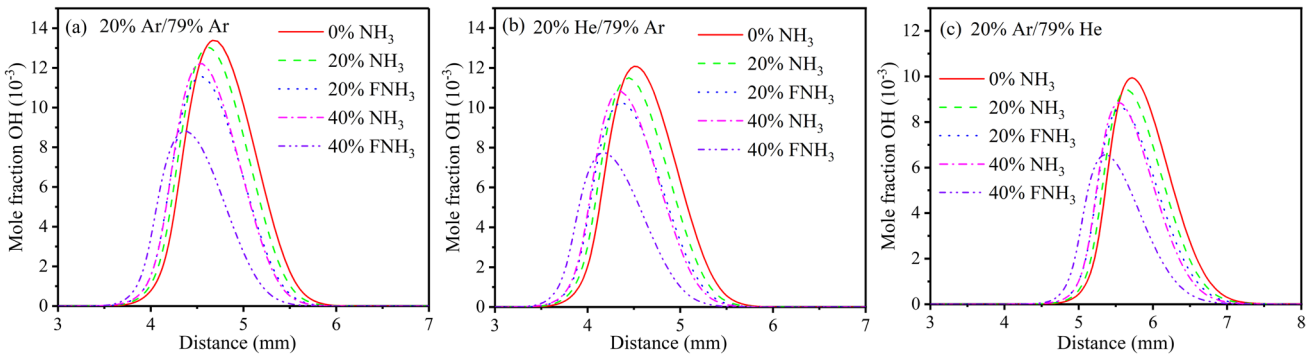

Fig. 6 Mole fraction profiles of OH with Ar or He dilution and different NH_3 additions

3.1.3 Intermediate hydrocarbon species

The intermediate hydrocarbon species would be oxidized with radicals to inhibit the soot formation to some extent. Therefore, the mole fractions of acetylene (C_2H_2), propynyl (C_3H_3), and benzene (A1), which were important soot precursors, in the combustion process of C_2H_4/NH_3 diluted with Ar (F1–F5 conditions in Table 1) or He (F6–F15 conditions in Table 1) were shown in Figs. 7, 8 and 9. It could be found that the combined effects of the NH_3 additive reduced the mole fractions of these important intermediate hydrocarbon species from Figs. 7a, 8a and 9a. The similar results had been achieved by Li et al. (2021), Shao et al. (2022) and Ren et al. (2022). In Fig. 7a, the differences between the mole distributions of C_2H_2 with NH_3 addition and FNH_3 addition demonstrated that the chemical effects of NH_3 promoted the

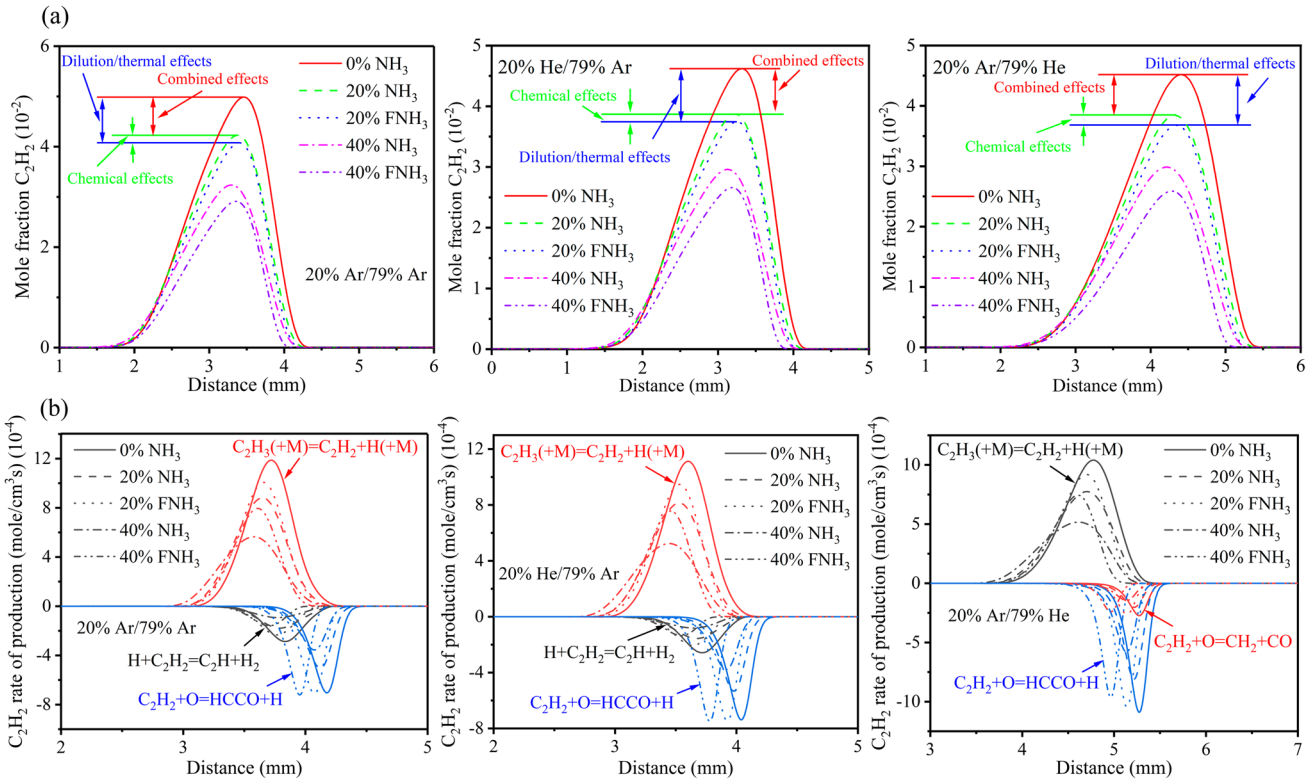

Fig. 7 Mole fractions and Rates of production of C_2H_2 with Ar or He dilution and different NH_3 additions. **a** Mole fractions; **b** Rates of production

formation of C_2H_2. Similarly, the chemical effects of NH_3 were also observed to increase the mole fractions of C_3H_3 and A1, as shown in subsequent Figs. 8a and 9a. Therefore, regardless of the dilution environment, the productions of C_2H_2, C_3H_3, and A1 were inhibited due to the dilution and thermal effects of NH_3, instead of the chemical effects of NH_3. It was worth pointing out that, as shown in Figs. 8a and 9a, the mole fractions of C_3H_3 and A1 were much lower when He replaced Ar on the fuel side or oxidizer side (F6–F15 conditions in Table 1). It revealed that the pathway of A1 generated by small molecule C_3H_3 in the C_2H_4/NH_3 counter-flow diffusion flame was more easily susceptible to He.

To analyze the detailed formation and consumption of these important intermediate hydrocarbon species, the rates of production were analyzed in Figs. 7b, 8b and 9b. It could be found that the main reaction concerning C_2H_2 formation was $C_2H_3(+M)=C_2H_2+H(+M)$, although the dilution environment was different, and the reaction rates were greatly reduced with the chemical effects of NH_3, as shown in Fig. 7b. Whereas the rate of the main reaction $C_2H_2+CH_2=C_3H_3+H$ for C_3H_3 formation was reduced mainly due to the dilution and thermal effects of NH_3, as shown in Fig. 8b. Figure 9b illustrated that the reaction $A1\text{-}+C_2H_4=A1+C_2H_3$ was mainly responsible for A1 formation, and the oxidation reaction $A1\text{-}+H(+M)=A1(+M)$ was added when He diluted on the fuel side. Comparing the NH_3 and FNH_3 additions, it could be found that the chemical effects of NH_3 promoted the reaction $A1\text{-}+C_2H_4=A1+C_2H_3$, whereas it suppressed other reactions.

3.2 With CO_2 dilution

When CO_2 was used as the diluent, the chemical effects of NH_3 may be influenced by the chemical effects of CO_2. Therefore, this section would put a special emphasis on the analysis of the coupled chemical effects of NH_3 and CO_2 on flame temperature, major species, free radicals, important intermediate hydrocarbon species, and oxygenated species.

3.2.1 Flame temperature profiles

As shown in Fig. 10, the addition of NH_3 reduced the flame temperature. In Fig. 10a, the differences between CO_2/NH_3 and CO_2/FNH_3 revealed that the chemical effects of NH_3 increased the temperature. The differences between CO_2/NH_3 and FCO_2/FNH_3 additions suggested that the coupled chemical effects of NH_3 and CO_2 also led to an increase in the flame temperature. However, with

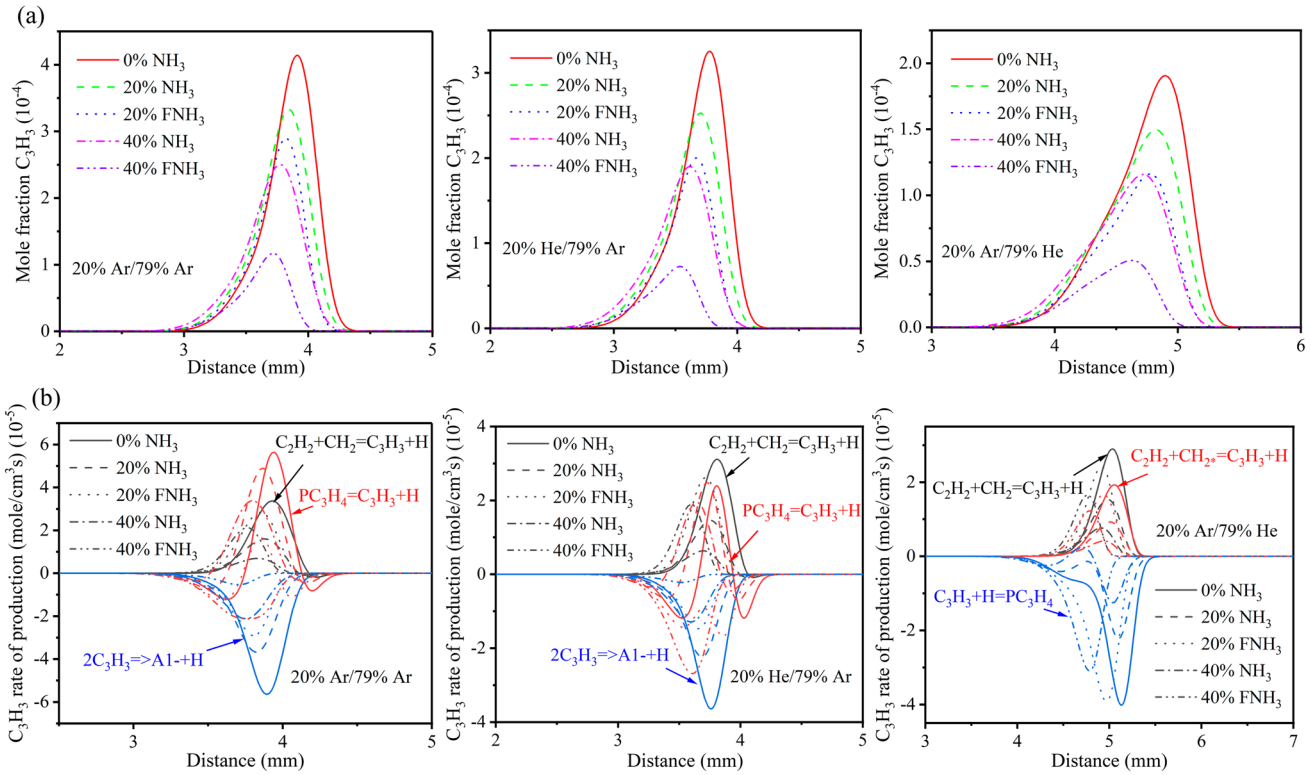

Fig. 8 Mole fractions and Rates of production of C_3H_3 with Ar or He dilution and different NH_3 additions. **a** Mole fractions; **b** Rates of production

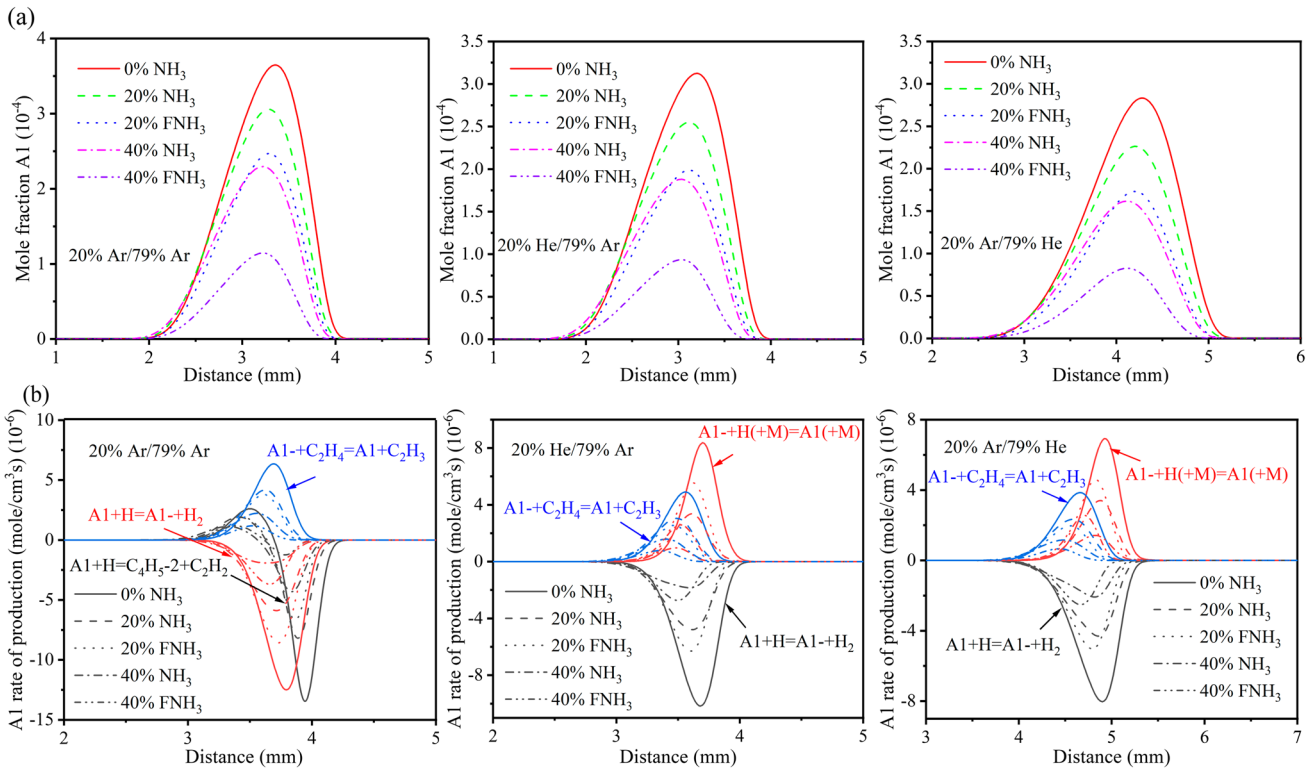

Fig. 9 Mole fractions and Rates of production of A1 with Ar or He dilution and different NH_3 additions. **a** Mole fractions; **b** Rates of production

CO_2 addition on the oxidizer side, as shown in Fig. 10b, the coupled chemical effects decreased the temperature. This was possibly because the chemical effects of CO_2 lowered the temperature (Liu et al. 2001) and were dominant with oxidizer-side addition. Meanwhile, it was worth noting that the temperature was greatly lower with the oxidizer-side CO_2 addition. Even when the condition was 40% NH_3/79% CO_2 (F15 condition in Table 2), the fuel could not be ignited. Therefore, the working condition would not be discussed in the following. As the known literature data showed that the threshold local temperature for the onset of soot formation in diffusion flames, T_c,

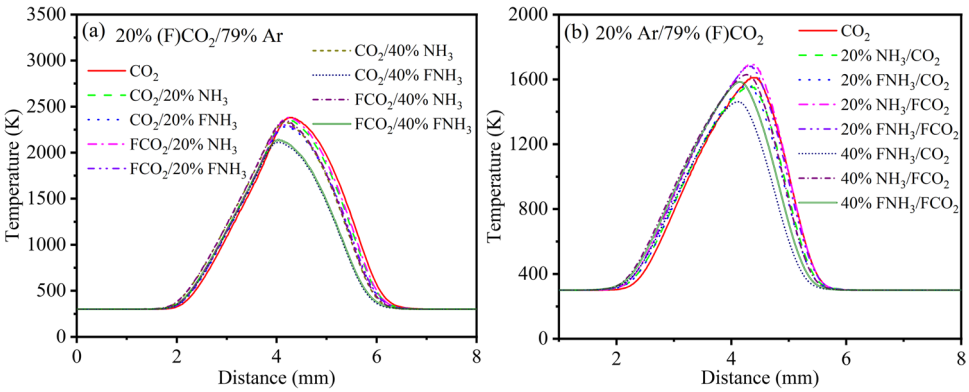

Fig. 10 Flame temperature with CO_2 dilution and different NH_3 additions. *Notes*: The 20% (F)CO_2/79% Ar and the 20% Ar/79% (F)CO_2 respectively represented dilution gas CO_2 replaced Ar on the fuel side (F1-F9 conditions in Table 2) and the oxidizer side (F10-F18 conditions in Table 2). The (F)CO_2 represented the normal CO_2 (CO_2) or fiction CO_2 (FCO_2) addition. The annotations for Figs. 11, 12, 13, 14, 15, 16 and 18 have the same meanings, which will not be noted again in the following

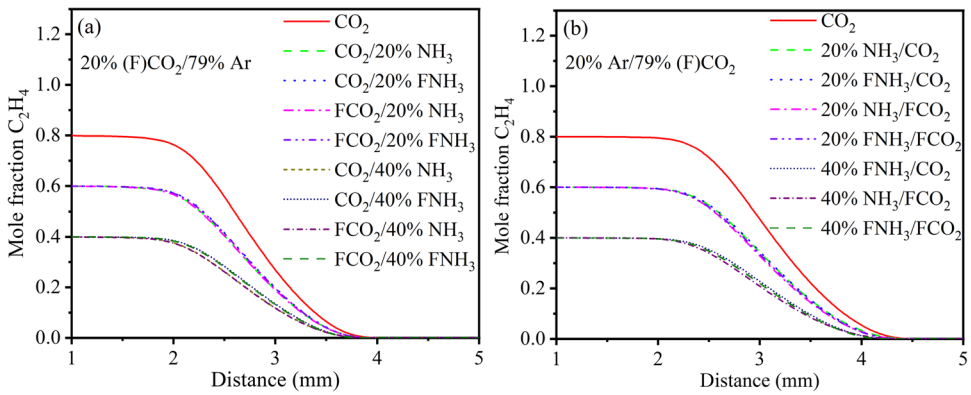

Fig. 11 Mole fraction profiles of C_2H_4 with CO_2 dilution and different NH_3 additions

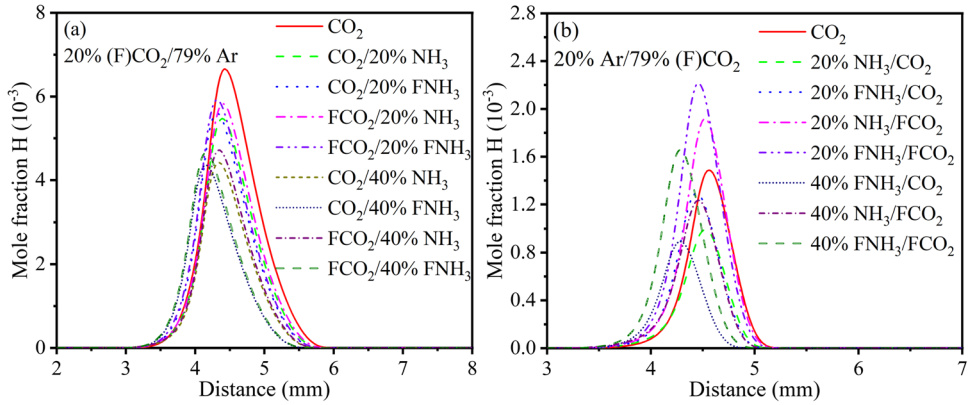

Fig. 12 Mole fraction profiles of H with CO_2 dilution and different NH_3 additions

satisfied the condition $T_c > 1300–1500$ K (Frolov et al. 2023), the analysis of soot precursors concentrations in flame conditions were necessary.

3.2.2 Major species and radicals

Figure 11 gave the mole fraction profiles of C_2H_4. The comparison with the addition of 40% NH_3 and 40% FNH_3 illustrated that the chemical effects of NH_3 reduced the C_2H_4 mole fraction slightly. However, the coupled effects of NH_3 and CO_2 on C_2H_4 were less pronounced when CO_2 is added to either the fuel side or the oxidizer side.

The mole fraction profiles of H radical were displayed in Fig. 12. It illustrated that the addition of NH_3 decreased the H concentration. The fuel-side CO_2 dilution (F1–F9 conditions in Table 2) was similar to the condition of Ar-diluted, the chemical effects of NH_3 reduced H concentration with 20% NH_3 addition, while increased the mole fraction of H when the blending ratio was 40%, as shown in Fig. 12a. Whereas, Fig. 12b illustrated that the chemical effects of NH_3 inhibit H formation with oxidizer-side CO_2 dilution (F10–F18 conditions in Table 2). The differences between the H radical of 20% CO_2/NH_3 and 20% FCO_2/NH_3 were owing to the chemical effects of CO_2, which could decrease the mole fraction of H radical This was the same result as the known literature (Liu 2015a). Moreover, the differences between NH_3/CO_2 and FNH_3/FCO_2 additions revealed that the reductions in H concentration were due to the coupled chemical effects of NH_3 and CO_2, especially with the oxidizer-side CO_2 addition. The existing literature (Liu et al. 2001; Mahmoud et al. 2019) indicated that in ethylene counter-flow diffusion flames, the flame sheet front was situated on the oxidizer side of the stagnation plane. Consequently, the addition of oxidizer may result in a more pronounced increase in the CO_2 concentrations at the flame sheet. The promotion of the $CO_2+H=CO+OH$ reaction was also more significant for the oxidizer side addition.

Figure 13 illustrated the mole fraction profiles of O radical. Similar to the reduction of the mole fractions of H radical, the coupled chemical effects of NH_3 and CO_2 reduced O radical concentration, especially with the addition of CO_2 on the oxidizing side.

However, the coupled chemical effects of NH_3 and CO_2 on the mole fraction of OH radical were different. As shown in Fig. 14a, the differences between NH_3/CO_2 and FNH_3/FCO_2 additions revealed that the coupled chemical effects of NH_3 and CO_2 promoted the formation of OH with fuel-side CO_2 addition. Nevertheless, the coupled chemical effects had obvious inhibitory effects when CO_2 addition on the oxidizer side, which were shown in Fig. 14b. It was possibly

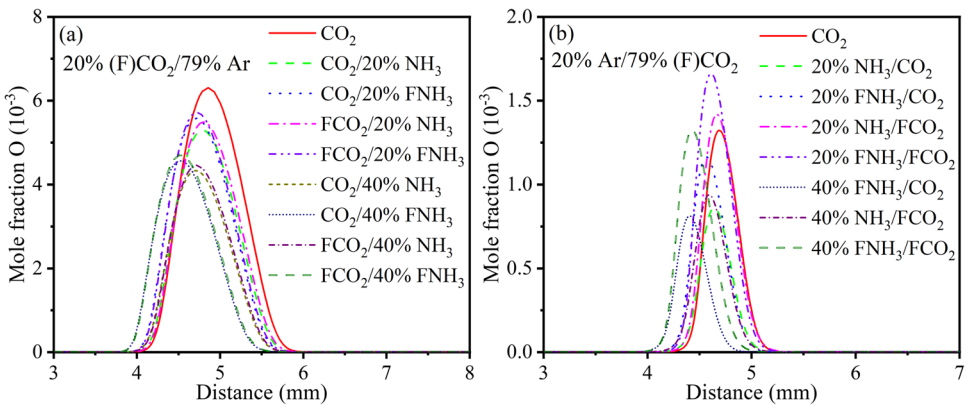

Fig. 13 Mole fraction profiles of O with CO_2 dilution and different NH_3 additions

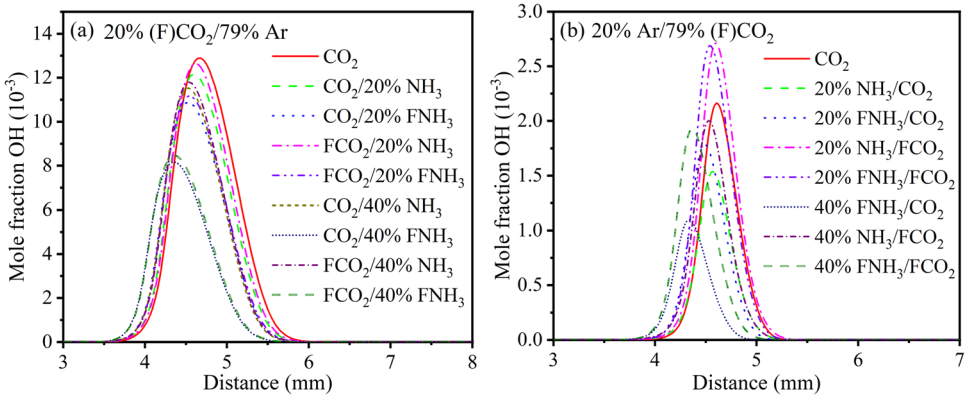

Fig. 14 Mole fraction profiles of OH with CO_2 dilution and different NH_3 additions

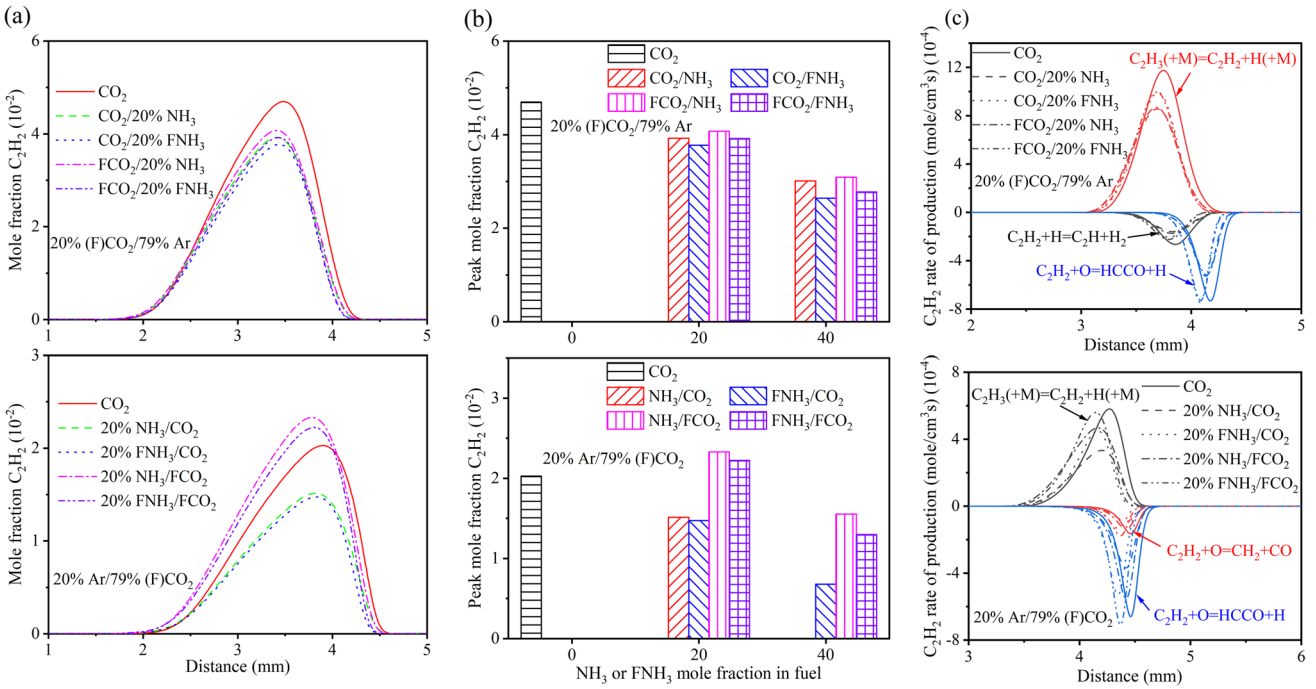

Fig. 15 Mole fractions and Rates of production of C_2H_2 with CO_2 dilution and different NH_3 additions. **a** Mole fractions; **b** Peak mole fractions; **c** Rates of production

because the chemical effects of CO_2 also decreased the OH radical mole fractions, which could be found from the differences between NH_3/CO_2 and NH_3/FCO_2 additions. And with the oxidizer-side CO_2 dilution, the chemical effects of CO_2 were more significant.

3.2.3 Intermediate hydrocarbon species

C_2H_2 was considered to be an important small molecule precursor of soot formation (Ruiz et al. 2007; Chernov et al. 2014; Wang and Chung 2019). C_3H_3 and A1 also were very vital for the soot production.

Firstly, the chemical effects of CO_2 and NH_3 on C_2H_2 concentration were identified in Fig. 15. The differences between CO_2/NH_3 and FCO_2/FNH_3 additions represented the coupled chemical effects of NH_3 and CO_2. Compared with Fig. 15a, b, it could be found that the coupled chemical effects of NH_3 and CO_2 were weak when CO_2 was from the fuel side (F1–F9 conditions in Table 2), while it led to a significant reduction in the mole fractions of C_2H_2 with

Table 4 The calculation of the chemical effects of NH_3 and CO_2 on the peak mole fraction of C_2H_2. Ai (i = 1, 2, 3) represented the chemical effects of NH_3, Bi (i = 1, 2, 3) represented the chemical effects of CO_2, Ai + Bi (i = 1, 2, 3) represented the sum of the separate chemical effects of NH_3 and CO_2, Ci (i = 1, 2, 3) represented the coupled chemical effects of NH_3 and CO_2

Case	(F)CO_2 (%)	(F)NH_3 (%)	Conditions	The difference of the peak mole fraction C_2H_2 (ppm)
A1	20	20	CO_2/NH_3-CO_2/FNH_3	1522.6
B1	20	20	CO_2/NH_3-FCO_2/NH_3	− 1469.8
A1 + B1	20	20		52.8
C1	20	20	CO_2/NH_3-FCO_2/FNH_3	35.7
A2	20	40	CO_2/NH_3-CO_2/FNH_3	3682.7
B2	20	40	CO_2/NH_3-FCO_2/NH_3	− 834.9
A2 + B2	20	40		2847.8
C2	20	40	CO_2/NH_3-FCO_2/FNH_3	2343.3
A3	79	20	NH_3/CO_2-FNH_3/CO_2	395.8
B3	79	20	NH_3/CO_2-NH_3/FCO_2	− 8167.0
A3 + B3	79	20		− 7771.2
C3	79	20	NH_3/CO_2-FNH_3/FCO_2	− 7095.6

CO_2 addition on the oxidizer side (F10–F18 conditions in Table 2). To discover C_2H_2 variation trends with increasing NH_3 additions, Fig. 15b gave the C_2H_2 peak mole fractions. It revealed explicitly that the coupled chemical effects of NH_3 and CO_2 increased the mole fractions of C_2H_2 more significantly with the concentration of NH_3 increasing, when CO_2 was added to the fuel side. Fig. 15c illustrated the rates of production analysis of C_2H_2, it could be found that the coupled chemical effects of NH_3 and CO_2 decreased the rate of the reaction $C_2H_3(+M)=C_2H_2+H(+M)$, which was the main reaction for C_2H_2 formation. Therefore, the participation of C_2H_2 in the growth reaction of polycyclic aromatic hydrocarbons (PAHs) through the HACA mechanism would be affected (Frenklach 2002), then the surface growth of soot could be inhibited to some extent.

According to the peak mole fractions of C_2H_2 shown in Fig. 15b and the calculation method shown in Table 4, the chemical effects of NH_3 and CO_2 could be demonstrated quantitatively (Pan and Liu 2017). In Table 4, Ai ($i=1, 2, 3$) represented the chemical effects of NH_3 in the combined effects of NH_3 and CO_2. Similarly, Bi ($i=1, 2, 3$) denoted the chemical effects of CO_2, Ai + Bi ($i=1, 2, 3$) represented the sum of the separate chemical effects of NH_3 and CO_2, Ci ($i=1, 2, 3$) was equal to the coupled chemical effects of NH_3 and CO_2. In the results of the calculation, a positive value indicated an increase and a negative value represented a decrease. When the condition was 40% NH_3/79% CO_2 (F15 condition in Table 2), the fuel could not be ignited, so only the coupled chemical effects of adding 20% NH_3 were considered with CO_2 addition on the oxidizer side. The B1, B2, B3 revealed that the chemical effects of CO_2 suppressed the formation of C_2H_2, which was consistent with the known literature (Liu et al. 2001; Liu 2015a), whereas the chemical effects of NH_3 increased the mole fractions of C_2H_2. The former dominated the latter and the net effects were to reduce the mole fractions of C_2H_2 with the oxidizer-side CO_2 addition, different from CO_2 addition on the fuel side. Compared with the (Ai + Bi) and Ci, it could be found that the changes of C_2H_2 mole fractions in the simultaneous presence of chemical effects of NH_3 and CO_2 were slightly smaller than the sum of the separate chemical effects of NH_3 and CO_2. It suggested that chemical interactions between the dopants were negligible, as the results of Mahmoud et al. (2019).

Figure 16 illustrated the mole fraction profiles and the rates of production of C_3H_3. From Fig. 16a, it could be concluded that the addition of NH_3 reduced the mole fractions of C_3H_3. The differences between NH_3/CO_2 and FNH_3/FCO_2 revealed that the coupled chemical effects of NH_3 and CO_2 increased the concentration of C_3H_3 with CO_2 addition on the fuel side (F1–F9 conditions in Table 2), contrary to the results of the oxidizer-side CO_2 addition (F10–F18 conditions in Table 2). Figure 16b illustrated that C_3H_3 was generated in large quantities by the complex reactions of $C_2H_2+CH_2$, which was one of the reasons why C_3H_3 was considered as the main precursor of A1 generated by small molecules (Jin et al. 2015), then PAHs were easy to form soot after physical or chemical coalesce. When

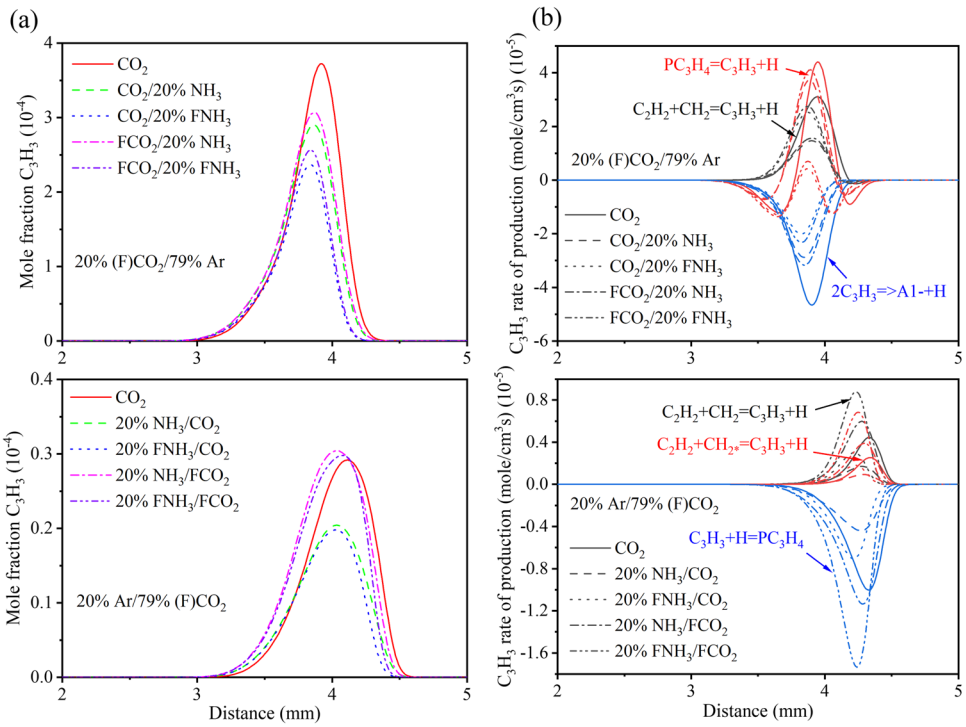

Fig. 16 Mole fractions and Rates of production of C_3H_3 with CO_2 dilution and different NH_3 additions. **a** Mole fractions; **b** Rates of production

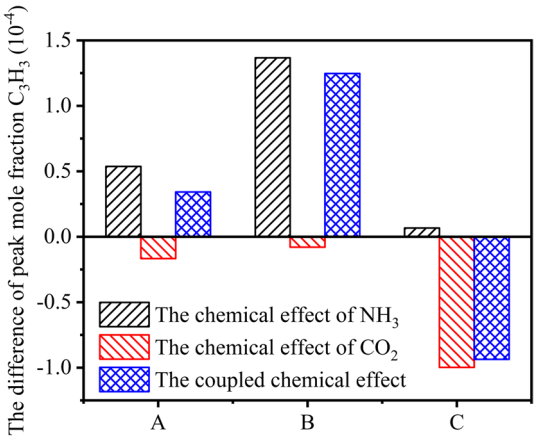

Fig. 17 The Difference of peak mole fractions of C_3H_3. *Notes*: A represented the fuel side was 60% C_2H_4 + 20% CO_2 + 20% NH_3, the oxidizer side was 79% Ar + 21% O_2; B represented the fuel side was 40% C_2H_4 + 20% CO_2 + 40% NH_3, the oxidizer side was 79% Ar + 21% O_2; C represented the fuel side was 60% C_2H_4 + 20% Ar + 20% NH_3, the oxidizer side was 79% CO_2 + 21% O_2. The positive results represented an increase and the negative results represented a decrease. The letters in Figs. 19 and 20 have the same meanings, which will not be noted again in the following.

CO_2 was added to the oxidizer side, the coupled chemical effects of NH_3 and CO_2 decreased the rates of all reactions, whereas CO_2 was from the fuel side, the rates of reactions $PC_3H_4 = C_3H_3 + H$ and $2C_3H_3 => A1- + H$ were decreased mainly due to the coupled dilution and thermal effects of NH_3 and CO_2. The bar plot of the chemical effects of NH_3 and CO_2 on the peak mole fractions of C_3H_3 was shown in Fig. 17. The formation of C_3H_3 was inhibited mainly because of the chemical effects of CO_2, Zhang et al. (2018) also gave the similar results, while the chemical effects of NH_3 promoted the formation of C_3H_3. When CO_2 was added to the oxidizer side, the coupled chemical effects of NH_3 and CO_2 could inhibit the generation of C_3H_3 due to the dominance of the chemical effects of CO_2, different from the fuel-side CO_2 addition.

It was generally agreed that PAHs were the precursors of soot formation, and the unique chemical structure of benzene ring (A1) was a prominent factor (Dobbins 2007). Therefore, it was necessary to analyze the variations of A1 concentration. The mole fraction profiles of A1 performed in Fig. 18a revealed that the normal NH_3 addition could cause the decrease of A1 mole fractions. However, the coupled chemical effects of NH_3 and CO_2 on the mole fraction of A1 were different due to the diverse sides and concentrations of CO_2 addition. With the fuel-side CO_2 addition (F1–F9 conditions in Table 2), the differences between CO_2/NH_3 and FCO_2/FNH_3 additions suggested that the coupled chemical effects of NH_3 and CO_2 increased the A1 mole fractions, in contradiction with adding CO_2 to the oxidizer side. Meanwhile, comparing the two situations, it could be found that the concentration of A1 was much lower when CO_2 was added to the oxidizer side (F10–F18 conditions in Table 2).

To analyze the detailed formation and consumption of A1, Fig. 18b gave the rates of production of A1. It could be found that the main reactions responsible for A1 formation were the closed-loop reactions $2C_3H_3 => A1$ and $C_2H_2 + C_4H_5\text{-}2 = A1 + H$. The main reactions

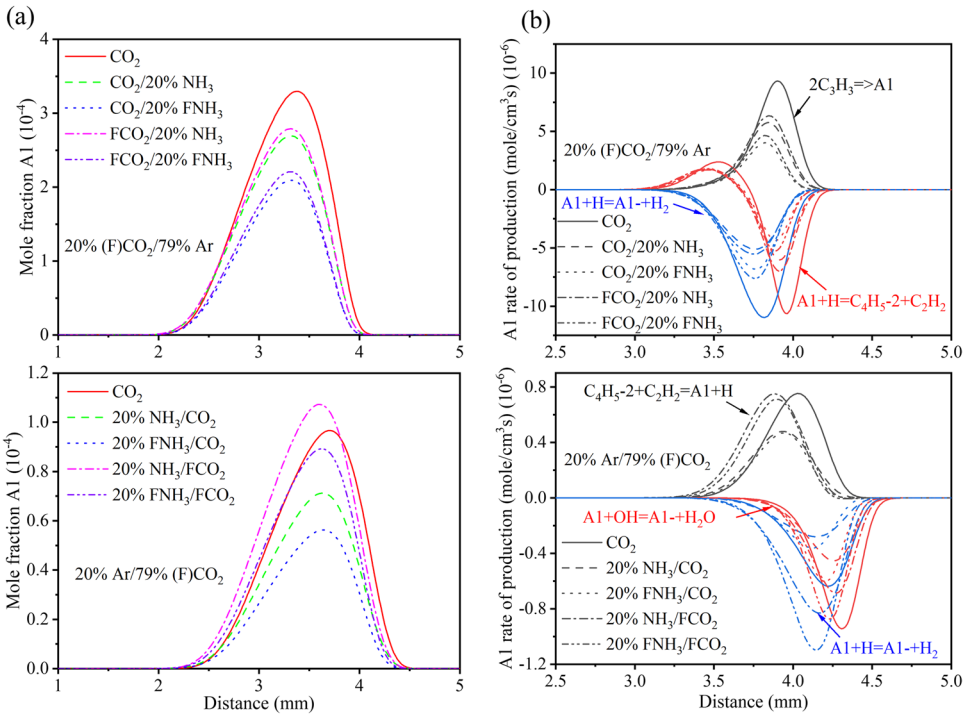

Fig. 18 Mole fractions and Rates of production of A1 with CO_2 dilution and different NH_3 additions. **a** Mole fractions; **b** Rates of production

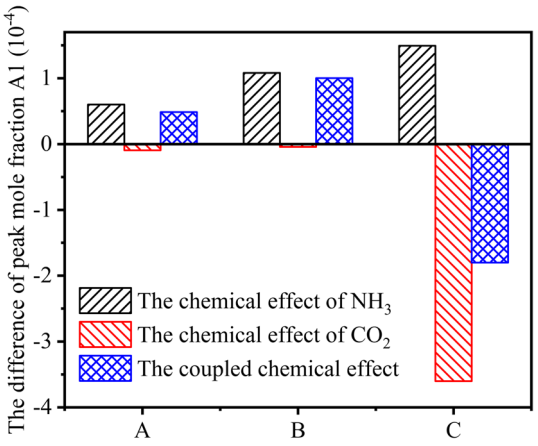

Fig. 19 The Difference of peak mole fractions of A1

responsible for A1 consumption were A1 + H = A1- + H_2, A1 + H = C_4H_5-2 + C_2H_2, and A1 + OH = A1- + H_2O. The pyrolysis consumption paths were mainly through hydrogen extraction reaction attacked by H radical (Yang et al. 2015). Comparing with CO_2/NH_3 and FCO_2/FNH_3 additions, it could be concluded that the reduced rates of all reactions were due to the coupled chemical effects of NH_3 and CO_2 with the oxidizer-side CO_2 addition. While adding CO_2 to the fuel side, the rate of reactions $2C_3H_3$=>A1 and A1 + H = C_4H_5-2 + C_2H_2 were decreased mainly because of the coupled dilution and thermal effects of NH_3 and CO_2.

By distinguishing the chemical effects of NH_3 and CO_2, as shown in Fig. 19, it could be found that the chemical effects of NH_3 promoted the generation of A1, while the chemical effects of CO_2 suppressed it. The results tied well with previous study (Naseri et al. 2017). Therefore, the coupled chemical effects of NH_3 and CO_2 on A1 mole fractions depended on the dominant effects. With the oxidizer-side CO_2 addition, the chemical effects of CO_2 dominated the chemical effects of NH_3, then the coupled chemical effects of NH_3 and CO_2 decreased the mole fraction of A1. For fuel-side CO_2 addition, the chemical effects of NH_3 on the A1 mole fraction were more significant and then the coupled chemical effects of NH_3 and CO_2 increased A1 concentration.

As the known literature (Liu et al. 2015), the chemical effect of CO_2 on soot loading reduction was primarily through reducing the rates of soot formation steps, rather than prompting soot oxidation. Therefore, with the addition of CO_2 on the oxidizer side, the coupled chemical effects of NH_3 and CO_2, which were mainly influenced by the chemical effect of CO_2, reduced both the mole fractions of O, H, OH radicals, and C_2H_2, C_3H_3, A1 soot precursors.

3.2.4 Intermediate oxygenated species

In addition to intermediate hydrocarbon species, intermediate oxygenated species such as formaldehyde (CH_2O) and acetaldehyde (CH_3CHO) were also important aldehyde contaminants generated in the combustion of hydrocarbon fuels. Formaldehyde was particularly irritant to the respiratory system and eyes, toxic and carcinogenic and could accelerate the production of the harmful substance ozone (Konnov et al. 2021). Therefore, the mole fraction profiles of CH_2O and CH_3CHO in C_2H_4/NH_3 flames with diluents were necessary to be revealed in Fig. 20.

Due to the chemical effects of CO_2, the chemical effects of NH_3 performed diverse impacts on CH_2O and CH_3CHO concentrations with different side CO_2 additions. Figure 20a illustrated that the coupled chemical effects of NH_3 and CO_2 decreased the mole fractions of CH_2O with the fuel-side CO_2 addition slightly (F1–F9 conditions in Table 2), whereas for the oxidizer side (F10–F18 conditions in Table 2), the coupled chemical effects promoted CH_2O formation. It could be explained that the chemical effects of CO_2 promoted the formation of CH_2O, and the coupled chemical effects of NH_3 and CO_2 were mainly affected by the chemical effects of CO_2, leading to an

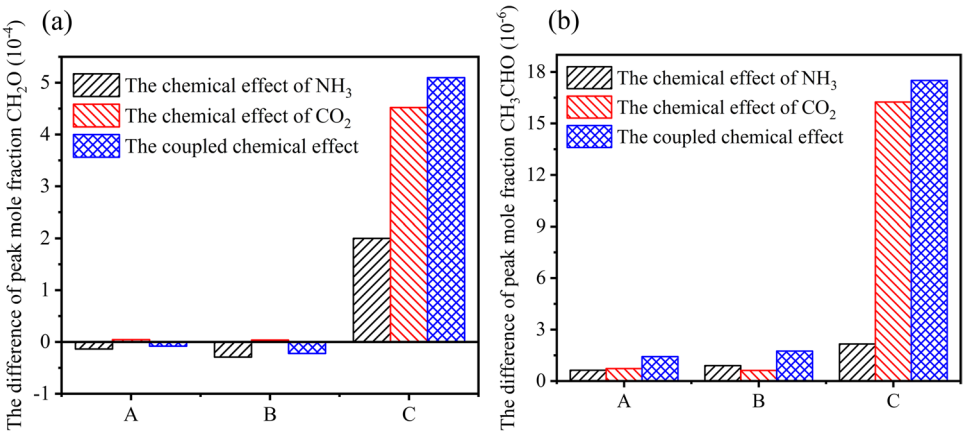

Fig. 20 The Difference of peak mole fractions of CH_2O and CH_3CHO. **a** CH_2O; **b** CH_3CHO

increase of the mole fraction of CH_2O with the oxidizer-side CO_2 addition.

Additionally, the chemical effects of NH_3 and CO_2 on the mole fraction of CH_3CHO were different from those of CH_2O. According to Fig. 20b, it could be found that the chemical effects of NH_3 promoted the formation of CH_3CHO, meanwhile, the coupled chemical effects of NH_3 and CO_2 further promoted the formation of CH_3CHO, especially when CO_2 was added to the oxidizer side.

4 Conclusions

The chemical kinetic analyses for the chemical effects of NH_3 with different diluents, in particular the coupled chemical effects of NH_3 and CO_2 in ethylene counter-flow diffusion flames, were investigated in this work. The analyses encompassed several critical aspects, such as flame temperature, major species, typical free radicals, intermediate hydrocarbon products, and oxygenated species. The outcomes of the study led to the following conclusions:

(1) Regardless of the diluents utilized, the flame temperature and the mole fractions of O, H, OH, C_2H_2, C_3H_3, A1 were decreased with NH_3 addition in C_2H_4/NH_3 counter-flow diffusion flames.
(2) With Ar or He dilution, the chemical effects of NH_3 promoted the formation of OH, C_2H_2, C_3H_3, and A1. With replacing Ar with He on the oxidizer side, the high thermal diffusivity of He reduced the flame temperature, and the pathway of A1 generated by small molecules C_3H_3 was more easily susceptible to He, leading to the lower concentrations of C_3H_3 and A1.
(3) With fuel-side CO_2 addition, the coupled chemical effects of NH_3 and CO_2 increased the flame temperature and the mole fractions of OH, C_2H_2, C_3H_3, A1. However, with oxidizer-side CO_2 addition, the coupled chemical effects, which were affected by the chemical effects of CO_2 significantly, inhibited the flame temperature and the formations of O, H, OH, C_2H_2, C_3H_3, A1.
(4) The chemical effects of NH_3 resulted in a decrease in the mole fraction of CH_2O and an increase in the concentration of CH_3CHO. The coupled chemical effects of NH_3 and CO_2 increased the CH_2O concentration with the oxidizer-side CO_2 addition.

Acknowledgements Authors thank the editor and reviewers' suggestions for improving the paper.

Author contributions ZMS: investigation, data curation, formal analysis, and writing-original draft; TTX: writing-review and editing; JYX, QGD, XZ, TJL, YYY: investigation; DL: methodology, supervision, writing-review and editing, supervision, project administration, and funding acquisition.

Funding This work was supported by the National Natural Science Foundation of China (52076110, 52106160), Jiangsu Provincial Natural Science Foundation of China (BK20200490, BK20220955) and the Fundamental Research Funds for the Central Universities (30923010208 and 30920031103).

Availability of data and materials Data will be available upon the request for authors.

Declarations

Competing interests The authors declare that they have no known competing financial interests or personal relationships that could have appeared to influence the work reported in this paper.

References

Abián M, Millera A, Bilbao R, Alzueta MU (2012) Experimental study on the effect of different CO_2 concentrations on soot and gas products from ethylene thermal decomposition. Fuel 91:307–312

Bennett AM, Liu P, Li ZP, Kharbatia NM, Boyette W, Masri AR, Roberts WL (2020) Soot formation in laminar flames of ethylene/ammonia. Combust Flame 220:210–218

Boyette WR, Steinmetz SA, Guiberti TF, Dunn MJ, Roberts WL, Masri AR (2021) Soot formation in turbulent flames of ethylene/hydrogen/ammonia. Combust Flame 226:315–324

Chen C, Liu D (2023) Review of effects of zero-carbon fuel ammonia addition on soot formation in combustion. Renewable Sustainable Energy Rev 185:113640

Chen C, Yang Q, Zhang R, Liu D. (2022) Regulation of organic hydrocarbon pollutants in coal volatiles combustion with CO_2 addition. J Cleaner Prod 374:133904.

Chernov V, Thomson MJ, Dworkin SB, Slavinskaya NA, Riedel U (2014) Soot formation with C1 and C2 fuels using an improved chemical mechanism for PAH growth. Combust Flame 161:592–601

Deng QG, Ying YY, Liu D (2022) Detailed chemical effects of ammonia as fuel additive in ethylene counterflow diffusion flames. Int J Hydrogen Energy 47:33498–33516

Dobbins RA (2007) Hydrocarbon nanoparticles formed in flames and diesel engines. Aerosol Sci Technol 41:485–496

Dong WL, Xiang LK, Gao J, Qiu BB, Chu HQ (2023) Effect of CO_2 dilution on laminar burning velocities, combustion characteristics

and NOx emissions of CH_4/air mixtures. Int J Coal Sci Technol 10(1):72. https://doi.org/10.1007/s40789-023-00655-9
Du DX, Axelbaum RL, Law CK (1990) The influence of carbon dioxide and oxygen as additives on soot formation in diffusion flames. Symp (Int) Combust 23:1501–1507
Frenklach M (2002) Reaction mechanism of soot formation in flames. Phys Chem Chem Phys 4:2028–2037
Frenklach M, Liu ZY, Singh RI, Galimova GR, Azyazov VN, Mebel AM (2018) Detailed, sterically-resolved modeling of soot oxidation: role of O atoms, interplay with particle nanostructure, and emergence of inner particle burning. Combust Flame 188:284–306
Frolov SM, Ivanov VS, Frolov FS, Vlasov PA, Axelbaum R, Irace PH, Yablonsky G, Waddell K (2023) Soot formation in spherical diffusion flames. Mathematics 11:261
Glarborg P, Miller JA, Ruscic B, Klippenstein SJ (2018) Modeling nitrogen chemistry in combustion. Prog Energy Combust Sci 67:31–68
Grcar JF, Glarborg P, Bell JB, Day MS, Loren A, Jensen AD (2004) Effects of mixing on ammonia oxidation in combustion environments at intermediate temperatures. Proc Combust Inst 30:1193–1200
Gu MY, Chu HQ, Liu FS (2016) Effects of simultaneous hydrogen enrichment and carbon dioxide dilution of fuel on soot formation in an axisymmetric co-flow laminar ethylene/air diffusion flame. Combust Flame 166:216–228
Guo HS, Smallwood GJ (2008) A numerical study on the influence of CO_2 addition on soot formation in an ethylene/air diffusion flame. Combust Sci Technol 180:1695–1708
Ichikawa A, Naito Y, Hayakawa A, Kudo T, Kobayashi H (2019) Burning velocity and flame structure of CH_4/NH_3/air turbulent premixed flames at high pressure. Int J Hydrogen Energy 44:6991–6999
Jin HF, Frassoldati A, Wang YZ, Zhang XY, Zeng MR, Li YY, Qi F, Cuoci A, Faravelli T (2015) Kinetic modeling study of benzene and PAH formation in laminar methane flames. Combust Flame 162:1692–1711
Kobayashi H, Hayakawa A, Somarathne KDKA, Okafor EC (2019) Science and technology of ammonia combustion. Proc Combust Inst 37:109–133
Konnov AA, Nilsson EJK, Christensen M, Zhou CW (2021) Combustion chemistry of methoxymethanol. Part II: Laminar flames of methanol + formaldehyde fuel mixtures. Combust Flame 229:111411
Lecoustre VR, Sunderland PB, Chao BH, Axelbaum RL (2012) Numerical investigation of spherical diffusion flames at their sooting limits. Combust Flame 159:194–199
Lhuillier C, Brequigny P, Lamoureux N, Contino F, Rousselle CM (2020) Experimental investigation on laminar burning velocities of ammonia/hydrogen/air mixtures at elevated temperatures. Fuel 263:116653
Li ZS, Han W, Liu D, Chen Z (2015) Laminar flame propagation and ignition properties of premixed iso-octane/air with hydrogen addition. Fuel 158:443–450
Li YP, Zhang YR, Zhan R, Huang Z, Lin H (2021) Experimental and kinetic modeling study of ammonia addition on PAH characteristics in premixed n-heptane flames. Fuel Process Technol 214:106682
Liu D (2014) Kinetic analysis of the chemical effects of hydrogen addition on dimethyl ether flames. Int J Hydrogen Energy 39:13014–13019
Liu D (2015a) Chemical effects of carbon dioxide addition on dimethyl ether and ethanol flames: a comparative study. Energy Fuels 29:3385–3393
Liu D (2015b) Detailed influences of ethanol as fuel additive on combustion chemistry of premixed fuel-rich ethylene flames. Sci China Technol Sci 58:1696–1704
Liu FS, Guo HS, Smallwood GJ, Gülder ÖL (2001) The chemical effects of carbon dioxide as an additive in an ethylene diffusion flame: implications for soot and NO_x formation. Combust Flame 125:778–787
Liu FS, Guo HS, Smallwood GJ (2003) The chemical effect of CO_2 replacement of N_2 in air on the burning velocity of CH_4 and H_2 premixed flames. Combust Flame 133:495–497
Liu D, Santner J, Togbé C, Felsmann D, Koppmann J, Lackner A, Yang XL, Shen XB, Ju YG, Kohse-Höinghaus K (2013) Flame structure and kinetic studies of carbon dioxide-diluted dimethyl ether flames at reduced and elevated pressures. Combust Flame 160:2654–2668
Liu FS, Karatas AE, Gülder ÖL, Gu MY (2015a) Numerical and experimental study of the influence of CO_2 and N_2 dilution on soot formation in laminar co-flow C_2H_4/air diffusion flames at pressures between 5 and 20 atm. Combust Flame 162:2231–2247
Liu Y, Cheng XB, Li Y, Qiu L, Wang X, Xu YS (2021) Effects of ammonia addition on soot formation in ethylene laminar diffusion flames. Fuel 292:120416
Luo MY, Liu D (2017) Kinetic analysis of ethanol and dimethyl ether flames with hydrogen addition. Int J Hydrogen Energy 42:3813–3823
Mahmoud NM, Yan FW, Zhou MX, Xu L, Wang Y (2019) Coupled effects of carbon dioxide and water vapor addition on soot formation in ethylene diffusion flames. Energy Fuels 33:5582–5596
Naseri A, Veshkini A, Thomson MJ (2017) Detailed modeling of CO_2 addition effects on the evolution of soot particle size distribution functions in premixed laminar ethylene flames. Combust Flame 183:75–87
Okafor EC, Naito Y, Colson S, Ichikawa A, Kudo T, Hayakawa A, Kobayashi H (2018) Experimental and numerical study of the laminar burning velocity of CH_4-NH_3-air premixed flames. Combust Flame 187:98–185
Park J, Hwang DJ, Choi JG, Lee KM (2003) Chemical effects of CO_2 addition to oxidizer and fuel streams on flame structure H_2–O_2 counterflow diffusion flames. Int J Energy Res 27:1205–1220.
Pan W, Liu D (2017) Coupled chemical effects of carbon dioxide and hydrogen additions on premixed lean dimethyl ether flames. Sci China Technol Sci 60:102–115
Ren F, Cheng XG, Gao Z, Huang Z, Zhu L (2022) Effects of NH_3 addition on polycyclic aromatic hydrocarbon and soot formation in C_2H_4 co-flow diffusion flames. Combust Flame 241:111958
Renard C, Dias V, Tiggelen PJV, Vandooren J (2009) Flame structure studies of rich ethylene-oxygen-argon mixtures doped with CO_2, or with NH_3, or with H_2O. Proc Combust Inst 32:631–637
Richter H, Howard JB (2000) Formation of polycyclic aromatic hydrocarbons and their growth to soot—a review of chemical reaction pathways. Prog Energy Combust Sci 26:565–608
Ruiz MP, Callejas A, Millera A, Alzueta MU, Bilbao R (2007) Soot formation from C_2H_2 and C_2H_4 pyrolysis at different temperatures. J Anal Appl Pyrolysis 79:244–251
Service RF (2018) Liquid sunshine. Science 316:120–123
Shao C, Campuzano F, Zhai YT, Wang HY, Zhang W, Sarathy SM (2022) Effects of ammonia addition on soot formation in ethylene laminar premixed flames. Combust Flame 235:111698
Shu B, He X, Ramos CF, Fernandes RX, Costa M (2021) Experimental and modeling study on the auto-ignition properties of ammonia/methane mixtures at elevated pressures. Proc Combust Inst 38:261–268
Sonker M, Tiwary SK, Shreyash N, Bajpai S, Ray M, Kar SK, Balathanigaimani MS (2022) Ammonia as an alternative fuel for

vehicular applications: paving the way for adsorbed ammonia and direct ammonia fuel cells. J Cleaner Prod 326:133960

Vancoillie J, Christensen M, Nilsson EJK, Verhelst S, Konnov AA (2013) The effects of dilution with nitrogen and steam on the laminar burning velocity of methanol at room and elevated temperatures. Fuel 105:732–738

Wang H (2011) Formation of nascent soot and other condensed-phase materials in flames. Proc Combust Inst 33:41–67

Wang Y, Chung SH (2019) Soot formation in laminar counterflow flames. Prog Energy Combust 74:152–238

Wang Y, Raj A, Chung SH (2013) A PAH growth mechanism and synergistic effect on PAH formation in counterflow diffusion flames. Combust Flame 160:1667–1676

Wang W, Xu L, Yan J, Wang Y (2020) Temperature dependence of the fuel mixing effect on soot precursor formation in ethylene-based diffusion flames. Fuel 267:117121

Wang Y, Gu MY, Wu JJ, Cao L, Lin YY, Huang XY (2021) Formation of soot particles in methane and ethylene combustion: a reactive molecular dynamics study. Int J Hydrogen Energy 46:36557–36568

Yang JZ, Zhao L, Yuan W, Qi F, Li YY (2015) Experimental and kinetic modeling investigation on laminar premixed benzene flames with various equivalence rations. Proc Combust Inst 35:855–862

Yelverton TLB, Roberts WL (2008) Soot surface temperature measurements in pure and diluted flames at atmospheric and elevated pressures. Exp Therm Fluid Sci 33:17–22

Ying YY, Liu D (2015) Detailed influences of chemical effects of hydrogen as fuel additive on methane flame. Int J Hydrogen Energy 40:3777–3788

Zamfirescu C, Dincer I (2009) Ammonia as a green fuel and hydrogen source for vehicular applications. Fuel Process Technol 90:729–737

Zhang YR, Wang LJ, Liu P, Guan B, Ni H, Huang Z, Lin H (2018) Experimental and kinetic study of the effects of CO_2 and H_2O addition on PAH formation in laminar premixed $C_2H_4/O_2/Ar$ flames. Combust Flame 192:439–451

Zhang K, Xu YS, Liu Y, Wang HK, Liu YM, Cheng XB (2023) Effects of ammonia addition on soot formation in ethylene laminar diffusion flames. Part 2. Further insights into soot inception, growth and oxidation. Fuel 331:125623

Zhao R, Liu D (2022) Temperature dependence of chemical effects of ethanol and dimethyl ether mixing on benzene and PAHs formation in ethylene counterflow diffusion flames. Energy 257:124809

Zhou SK, Yang WJ, Tan HZ, An QW, Wang JH, Dai HC, Wang XX, Wang XB, Deng SH (2021) Experimental and kinetic modeling study on NH_3/syngas/air and NH_3/bio-syngas/air premixed laminar flames at elevated temperature. Combust Flame 233:111594

Zhou MX, Yan FW, Ma LH, Jiang P, Wang Y, Chung SH (2022) Chemical speciation and soot measurements in laminar counterflow diffusion flames of ethylene and ammonia mixtures. Fuel 308:122003